

Distinction Between Cu^{2+} and Zn^{2+} Ions in a Crystal of Spinach Superoxide Dismutase by Use of Anomalous Dispersion and Tuneable Synchrotron Radiation

BY YASUYUKI KITAGAWA, NOBUO TANAKA, YASUO HATA AND YUKITERU KATSUBE

Institute for Protein Research, Osaka University, 3-2 Yamadaoka, Suita, Osaka 565, Japan

AND YOSHINORI SATOW

Photon Factory, National Laboratory for High Energy Physics, Oho-machi, Tsukuba-gun, Ibaraki 305, Japan

(Received 5 September 1986; accepted 23 October 1986)

Abstract

Cu^{2+} and Zn^{2+} ions in a single crystal of spinach superoxide dismutase have been distinguished by enhancing the anomalous-dispersion effect of each ion with a wavelength near its *K* absorption edge, though these metal ions were not distinguishable in the original native Fourier map. The X-ray diffraction data were collected on a four-circle diffractometer for protein crystallography using a focused tuneable synchrotron radiation source at the Photon Factory. Anomalous difference Fourier maps with the phases from the conventional structure analysis were calculated for the data sets at wavelengths of 1.373 and 1.389 Å near the Cu *K* absorption edge, and 1.275 and 1.299 Å near the Zn *K* absorption edge. A comparison of these maps made it possible to distinguish between the Cu^{2+} and Zn^{2+} ions, which have only a one-electron difference. This shows that metals or ions whose atomic numbers are close to one another may be located exactly by taking advantage of enhanced anomalous-dispersion data and reliable phase angles.

Introduction

Synchrotron radiation is being increasingly utilized for data collection of protein crystals owing to its brightness, parallelism and tuneability. It is worthwhile noting that anomalous-dispersion effects around specific absorption edges of bound metal ions can be optimized by finely tuning the synchrotron X-ray wavelength. In the case of proteins with more than one kind of metal cofactor, differences in both of the anomalous components f' and f'' can be used to distinguish atoms or ions with similar atomic numbers. Such differences have already been utilized to locate manganese and calcium cofactors, which have a five-electron difference, in a pea lectin crystal (Einspahr, Suguna, Suddath, Ellis, Helliwell & Pariz, 1985).

Spinach superoxide dismutase is composed of two identical subunits with 154 amino acid residues and

$M_r = 16\,000$ (Kitagawa, Tsunasawa, Tanaka, Katsube, Sakiyama & Asada, 1986). Each subunit contains both a Cu^{2+} and a Zn^{2+} ion. The enzyme crystallizes in space group *C2* with cell dimensions $a = 166.3$ (3), $b = 46.0$ (1), $c = 85.7$ (1) Å, $\beta = 99.4$ (1)°, and with two molecules or four identical subunits per asymmetric unit (Kitagawa, Tanaka, Katsube, Kusunoki, Lee, Morita, Asada & Aihara, 1984). The crystal structure of spinach superoxide dismutase has been determined at 2.0 Å resolution, and the details of the structure analysis will be published elsewhere. Synchrotron radiation from the Photon Factory vertical wiggler (Huke & Yamakawa, 1980) was used to locate the Cu^{2+} and Zn^{2+} ions unambiguously enhancing both the real coefficients f' and the imaginary coefficients f'' of each ion. Wavelengths for data collection were selected close to the Cu *K* edge at 1.380 Å and the Zn *K* edge at 1.283 Å (*International Tables for X-ray Crystallography*, 1974), because the f' and f'' values of the Cu^{2+} and Zn^{2+} ions show a pronounced change near the wavelength of their *K* absorption edge.

In the present study, the anomalous difference Fourier maps which mainly reflect the f'' effect of a specific atom or ion are compared with each other in order to locate metal ions and to distinguish between the Cu^{2+} ion and the Zn^{2+} ion in the superoxide dismutase molecule. The difference Fourier maps of the different data sets, which reflect the f' effect, are also examined; the results are in agreement with those of the anomalous difference Fourier calculations. This paper describes the usefulness of Fourier syntheses of the anomalous-scattering effects in distinguishing between the Cu^{2+} and Zn^{2+} ions.

Experimental

Five sets of intensity data of Bijvoet-pair reflections (F^+ and F^-) were measured up to 6 Å resolution at five different wavelengths where these data sets represent various anomalous-scattering effects of Cu^{2+} and Zn^{2+} ions, respectively. The five wavelengths were

Table 1. *Anomalous-dispersion intensities at different wavelengths*

Data set (λ , Å)	f'		f''	
	Cu	Zn	Cu	Zn
1·000	-0·1	-0·4	2·3	2·6
1·275	-1·7	-4·5	3·4	3·8
1·299	-2·0	-4·1	3·5	0·5
1·373	-4·8	-2·4	3·9	0·6
1·389	-4·8	-2·3	0·5	0·6

1·000, 1·275, 1·299, 1·373 and 1·389 Å, and the contributions of f' and f'' for each metal ion are summarized in Table 1 (Sasaki, 1984). The data set at $\lambda = 1·000$ Å is useful for the calculation of the difference Fourier maps of the other four data sets, because the f' effect at this wavelength is rather small compared with those at the other four wavelengths.

All the data were collected with a four-circle diffractometer using synchrotron radiation at the Photon Factory. The diffractometer was located on the station of the beam line 14A; it has a horizontal-type setup and utilizes the radiation from a superconducting vertical wiggler (Satow, 1984). The white X-ray beam, which has a higher degree of polarization in the vertical direction, is monochromatized by an Si(111) double-crystal monochromator and then focused by a Pt-coated fused-quartz mirror (Satow, 1984). Wavelength calibrations were made by measuring the absorption spectra of Cu and Zn foils at their K absorption edges. The intensity of the X-ray beam incident to the specimen was monitored by an ion chamber for every measurement in order to correct for intensity change (Satow, 1984). The raw data were corrected for Lorentz and polarization factors. The polarization factor was calculated, assuming that the X-ray beam incident to the monochromator was polarized 90% in the vertical direction. Three standard reflections were measured every 100 reflections and a damage correction was made from the decay of these reflections. An absorption correction was carried out based on the method of North, Phillips & Mathews (1968).

Results

As a first approach, an anomalous difference Fourier calculation was carried out to distinguish the two kinds of metal ions from each other. The Fourier syntheses for five different data sets obtained at $\lambda = 1·000, 1·275, 1·299, 1·373$ and $1·389$ Å were calculated by the method described by Kraut (1968). The phases of each reflection in the calculation were derived from the crystal structure analysis. The intensity differences in the structure-factor amplitudes between Bijvoet-pair reflections are primarily due to both Cu^{2+} and Zn^{2+} at $\lambda = 1·275$ Å, and mainly to Cu^{2+} at $\lambda = 1·299$ and $1·373$ Å (Table 1). At $\lambda = 1·389$ Å, the difference in the amplitude should be negligibly small.

Table 2. *Electron density values at the Cu^{2+} and the Zn^{2+} positions in the Fourier maps*

Data set (λ , Å)	Yellow		Violet		Green		Blue		HUP
	Cu	Zn	Cu	Zn	Cu	Zn	Cu	Zn	
N-2·8	26	37	25	29	34	29	30	40	—
N-2·5	66	86	65	93	67	94	63	92	—
1·000*†	30	90	62	59	90	75	32	74	123
1·275*	103	126	73	149	83	154	108	115	70
1·299*	101	35	63	30	109	18	96	40	73
1·373*	113	7	134	41	139	0	124	18	80
1·389*	20	9	25	54	27	17	53	19	77
1·275‡	14	1	8	34	11	41	24	4	86
1·299‡	12	0	0	28	17	29	8	0	83
1·373‡	56	0	32	17	68	22	61	0	81
1·389‡	30	0	21	22	66	27	49	0	75

* Anomalous difference Fourier maps.

† This anomalous difference Fourier map was calculated to investigate the signal-to-noise ratio.

‡ Difference Fourier maps with the 1·000 Å data set.

For the 1·275 Å data set, the positions of the eight prominent peaks in the asymmetric unit were identical to those of the two kinds of metal ions in the original native Fourier map, although the four peaks at the possible Zn^{2+} ion sites were slightly higher than the other four at the possible Cu^{2+} ion sites, as shown in Table 2. This is consistent with the fact that the anomalous-dispersion component f'' of a Zn^{2+} ion is larger than that of a Cu^{2+} ion by 0·4 as shown in Table 1. On this Fourier map, only the anomalous scatterers can be located and in fact only four Cu^{2+} and four Zn^{2+} ions in the asymmetric unit of the superoxide dismutase crystal showed anomalous-scattering effects at this wavelength, because the eight prominent peaks can be completely assigned to the Cu^{2+} and Zn^{2+} ion positions of four subunits in the asymmetric unit.

For the 1·299 and 1·373 Å data sets, anomalous difference Fourier maps showed almost the same electron density distributions around the eight metal-ion positions. They gave high electron density humps at four possible Cu^{2+} ion sites and almost flat density at four Zn^{2+} ion sites (Fig. 1, Table 2). This is consistent with the fact that the anomalous-dispersion component f'' of a Cu^{2+} ion is about seven times larger than that of a Zn^{2+} ion at these two wavelengths (Table 1).

For the 1·389 Å data set, at which there is little f'' contribution of Cu^{2+} and Zn^{2+} ions, no significant electron density humps were found in the anomalous difference Fourier map around the previous eight positions of metal ions. The highest peak in an asymmetric unit could not be assigned to the metal-ion positions. The ratio of the peak density at the possible

metal-ion position to the highest uninterpretable peak is lower than in the other three cases (Table 2).

As a second approach, the conventional difference Fourier calculation between the 1.000 Å data set and each data set of the other four wavelengths (1.275, 1.299, 1.373, 1.389 Å) was carried out with the same phase angles used in the previous approach. The Fourier coefficients were obtained by averaging the

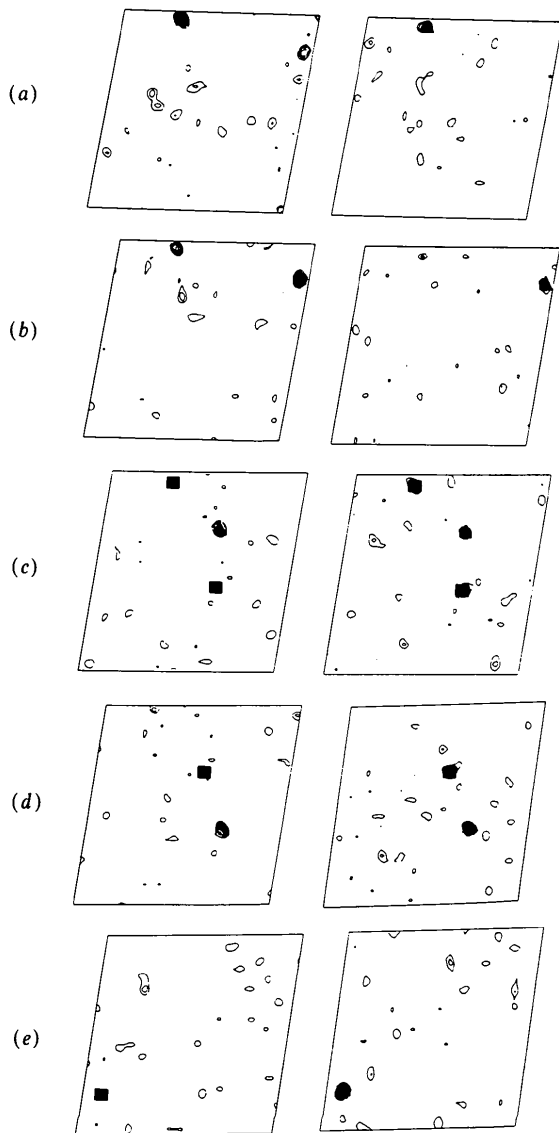


Fig. 1. Anomalous difference Fourier maps: left-hand side, 1.373 Å data set; right-hand side, 1.275 Å data set. The triangles are four Cu^{2+} ion positions and the squares are four Zn^{2+} ion positions in an asymmetric unit. The sections are (a) 4/50, (b) 6/50, (c) 13/50, (d) 17/50, and (e) 24/50 of the crystallographic b axis. At 4/50 and 6/50, the same peaks appear on the left-hand map. Contours are in equal intervals of positive density and are chosen to show the highest peak in each map with eight contour levels. The edges of the maps correspond to half the unit cell in a along the horizontal direction and the full unit cell in c along the vertical direction.

amplitudes of Bijvoet-pair reflections (F^+ and F^-) to take off the f'' contributions. The scaling factors between the different data sets were calculated by Wilson's statistics (Wilson, 1949). The results are summarized in Table 2. For the 1.373 and 1.389 Å data sets near the Cu K absorption edge, the difference maps gave significantly higher peaks at possible Cu^{2+} ion positions than those at possible Zn^{2+} ion positions, except for one case, the violet subunit in the 1.389 Å data set (see Table 2). On the other hand, for the 1.275 and 1.299 Å data sets near the Zn K absorption edge, the difference maps did not consistently give higher peaks at possible Zn^{2+} ion positions than those at possible Cu^{2+} ion positions. Each difference map was quite noisy compared with the anomalous difference Fourier map, and the highest peak in each map corresponds not to the position of a metal ion but to an uninterpretable peak. The quality of the difference Fourier map may suffer from errors in scaling between different data sets and in the different absorption effects from different crystals.

As a third approach to confirm the accuracy of the metal-ion positions, an anomalous difference Patterson synthesis was performed for each data set. This synthesis did not give any significant peaks which could be interpreted as Cu^{2+} or Zn^{2+} ions.

Discussion

Until now, distinction between two or more kinds of metal ions with similar atomic numbers has been dependent upon consideration of differences in the chemical nature of the ions. In the present study of spinach superoxide dismutase, however, the distinction between Cu^{2+} and Zn^{2+} ions, which have only a one-electron difference, has been achieved by using anomalous difference Fourier techniques based on reliable phase angles and intense tuneable synchrotron radiation. In particular, the anomalous difference Fourier maps of the 1.275, 1.299 and 1.373 Å data sets are very useful in distinguishing the ions from each other. On the map of the 1.275 Å data set, both the Cu^{2+} and Zn^{2+} ions appeared as the higher electron density humps, while only the Cu^{2+} ions were visible on the map of the 1.299 and 1.373 Å data sets. The map of the 1.373 Å data set gave a higher signal-to-noise ratio than that of the 1.299 Å data set. This is consistent with the fact that the former has a little higher contribution of f' and f'' than the latter, as shown in Table 1. It should be mentioned that the refined phase angles of each reflection play important roles in producing these kinds of results. In contrast to the success of the Fourier syntheses, an anomalous difference Patterson synthesis failed to locate the metal ions. Patterson syntheses may therefore be less powerful than anomalous difference Fourier syntheses in the case of a protein crystallographic

study, as was the case in another report (Cascarano, Giacobozzo, Peerdeman & Kroon, 1982). However, the ability to distinguish atoms or ions with only a one-electron difference in macromolecules such as proteins must be seen as a great advance in X-ray protein crystallography. This has been achieved by the development of an intense, tuneable synchrotron radiation source.

This work was supported in part by a Grant-in-Aid for Scientific Research (60470153) from the Ministry of Education, Science and Culture of Japan.

References

- CASCARANO, G., GIACOVAZZO, C., PEERDEMAN, A. F. & KROON, J. (1982). *Acta Cryst.* **A38**, 710-717.
- EINSPAHR, H., SUGUNA, K., SUDDATH, F. L., ELLIS, G., HELLIWELL, J. R. & PARIZ, M. Z. (1985). *Acta Cryst.* **B41**, 336-341.
- HUKE, K. & YAMAKAWA, T. (1980). *Nucl. Instrum. Methods*, **177**, 253-257.
- International Tables for X-ray Crystallography* (1974). Vol. IV, pp. 171. Birmingham: Kynoch Press. (Present distributor D. Reidel, Dordrecht.)
- KITAGAWA, Y., TANAKA, N., KATSUBE, Y., KUSUNOKI, M., LEE, G. P., MORITA, Y., ASADA, K. & AIHARA, D. (1984). *Acta Cryst.* **A40**, C43.
- KITAGAWA, Y., TSUNASAWA, S., TANAKA, N., KATSUBE, Y., SAKIYAMA, F. & ASADA, K. (1986). *J. Biochem.* **99**, 1289-1298.
- KRAUT, J. (1968). *J. Mol. Biol.* **35**, 511-512.
- NORTH, A. C. T., PHILLIPS, D. C. & MATHEWS, F. S. (1968). *Acta Cryst.* **A24**, 351-359.
- SASAKI, S. (1984). *Anomalous Scattering Factors for Synchrotron Users, Calculated Using Cromer and Liberman's Method*. National Laboratory for High Energy Physics, Ibaraki, Japan.
- SATOW, Y. (1984). In *Methods and Applications in Crystallographic Computing*, edited by S. R. HALL & T. ASHIDA, pp. 56-64. Oxford Univ. Press.
- WILSON, A. J. C. (1979). *Acta Cryst.* **2**, 318-321.

Acta Cryst. (1987). **B43**, 275-280

A Statistical Stereochemical Model of the Flexible Furanose Ring

BY V. N. BARTENEV, N. G. KAMENEVA AND A. A. LIPANOV

Institute of Molecular Genetics, USSR Academy of Sciences, Kurchatov Sq., 46, Moscow 123182, USSR

(Received 27 November 1985; accepted 1 December 1986)

Abstract

The probabilities of alternative conformations of the furanose ring in nucleosides and nucleotides and the free-energy difference have been determined from statistical analysis of X-ray data. Approximate analytical expressions have been obtained defining the optimal one-parameter pathway of conformational changes for furanose.

Introduction

Furanose rings, which enter into the sugar-phosphate backbone of nucleic acids, possess a considerable conformational flexibility; the configurations assumed by the rings are important stereochemical characteristics of the three-dimensional structure of DNA and RNA molecules. Any description of the stereochemistry of furanose is rendered difficult by the fact that in order to simulate the conformational rearrangements of the ring one has to allow for the changing valence angles and bonds (Westhof & Sundaralingam, 1980; Pearlman & Kim, 1985). A complete description of the configuration of the five-membered flexible ring would mean defining nine

($5 \times 3 - 6$) parameters, which is superfluous in many practical cases.

For a more economic description of the ring configuration, one can use the parameters of pseudorotation: phase angle P and pseudorotation amplitude τ_m (Altona & Sundaralingam, 1972). The furanose ring structures known from X-ray diffraction are distributed in the conformational range of the parameters P , τ_m close to the pseudorotation pathway with a roughly constant value $\tau_m \approx 39^\circ$ (Murray-Rust & Motherwell, 1978; Westhof & Sundaralingam, 1980), i.e. this is the most probable pathway for the conformational changes of furanose. The experimental data have been approximated to obtain analytical expressions (regression curves) for the ring's valence angles as functions of P along the pseudorotation pathway (Murray-Rust & Motherwell, 1978; Westhof & Sundaralingam, 1980). However, the use of these expressions for a one-parameter definition of the furanose conformation does not ensure the optimal stereochemistry of the ring as a whole, since the approximation coefficients were chosen for each individual angle regardless of the others and without stereochemical limitations. Even the simplest limitation, viz the condition of ring closure, alters the